

Magnetic loops in the quiet Sun

T. WIEGELMANN¹, S. K. SOLANKI^{1,8}, J. M. BORRERO², V. MARTÍNEZ PILLET³,
J. C. DEL TORO INIESTA⁴, V. DOMINGO⁵, J. A. BONET³, P. BARTHOL¹,
A. GANDORFER¹, M. KNÖLKER⁶, W. SCHMIDT², & A. M. TITLE⁷

¹*Max-Planck-Institut für Sonnensystemforschung, Max-Planck-Str. 2, 37191 Katlenburg-Lindau, Germany.*

²*Kiepenheuer-Institut für Sonnenphysik, Schöneckstr. 6, 79104 Freiburg, Germany.*

³*Instituto de Astrofísica de Canarias, C/Via Láctea s/n, 38200 La Laguna, Tenerife, Spain.*

⁴*Instituto de Astrofísica de Andalucía (CSIC), Apartado de Correos 3004, 18080 Granada, Spain.*

⁵*Grupo de Astronomía y Ciencias del Espacio, Universidad de Valencia, 46980 Paterna, Valencia, Spain.*

⁶*High Altitude Observatory, National Center for Atmospheric Research, Boulder, CO 80307, USA. The National Center for Atmospheric Research is sponsored by the National Science Foundation.*

⁷*Lockheed Martin Solar and Astrophysics Laboratory, Bldg. 252, 3251 Hanover Street, Palo Alto, CA 94304, USA.*

⁸*School of Space Research, Kyung Hee University, Yongin, Gyeonggi, 446-701, Korea.*

wiegelmann@mps.mpg.de

ABSTRACT

We investigate the fine structure of magnetic fields in the atmosphere of the quiet Sun. We use photospheric magnetic field measurements from SUNRISE/IMaX with unprecedented spatial resolution to extrapolate the photospheric magnetic field into higher layers of the solar atmosphere with the help of potential and force-free extrapolation techniques. We find that most magnetic loops which reach into the chromosphere or higher have one foot point in relatively strong magnetic field regions in the photosphere. 91% of the magnetic energy in the mid chromosphere (at a height of 1 Mm) is in field lines, whose stronger foot point has a strength of more than 300 G, i.e. above the equipartition field strength with convection. The loops reaching into the chromosphere and corona are also found to be asymmetric in the sense that the weaker foot point has a strength $B < 300$ G and is located in the internetwork. Such loops are expected to be strongly dynamic and have short lifetimes, as dictated by the properties of the internetwork fields.

Subject headings: Sun: magnetic topology—Sun: chromosphere—Sun: corona—Sun: photosphere

1. Introduction

The Sun's magnetic field lies at the heart of the heating of the solar corona and the solar chromosphere (with the possible exception of the basal flux; see, e.g., Bello González et al. 2010). Unfortunately, however, the magnetic field is measured almost exclusively in the solar photosphere and needs to be extrapolated from there in order to obtain its structure in the Sun's upper atmosphere. The balloon-borne SUNRISE mission (Solanki et al. 2010; Barthol et al. 2010) ob-

tained the magnetic field in the quiet solar photosphere with a very high and homogeneous spatial resolution. This allows us to investigate the 3D structure of the quiet Sun's magnetic field in more detail as compared with SOHO (e.g. Wiegelmann & Solanki 2004; He et al. 2007) or Hinode (e.g. Martínez González & Bellot Rubio 2009; Martínez González et al. 2010).

The resolution of the extrapolated field in the vertical direction depends on the spatial scales of the photospheric measurements. With a pixel size of 40 km on the Sun and a spatial resolution of

~ 100 km, we can, for the first time, resolve the thin layer of the photosphere and the lower chromosphere with several grid points. This allows us to study the magnetic connectivity between photosphere, chromosphere and corona by well-resolved magnetic loops. We also briefly discuss the possible implications of our results for quiet Sun loop heating models. This is of particular interest due to the large number of horizontal magnetic features in the photosphere, many of them associated with emerging magnetic loops (Martínez González et al. 2008; Danilovic et al. 2010) and the lack of acoustic wave energy flux proposed by Carlsson et al. (2007) which inspires us to consider alternatives, although the recent work by Bello González et al. (2009, 2010) suggests that the acoustic energy flux may well have been underestimated in the past due to insufficient spatial resolution.

2. Extrapolation of photospheric magnetic field measurements into the upper solar atmosphere

Here we use a (phase diversity reconstructed) Stokes vector map of a 37×37 Mm quiet Sun region in the photosphere recorded by SUNRISE/IMaX (Martínez Pillet et al. 2010, the data set was observed for 1.616 hours starting at 00:00 UT on 2009 June 9th.). The magnetic vector is obtained by inverting these data using the VFISV code by Borrero et al. (2010). We take 200 km as the average height at which the Fe I spectral line at 5250.2 \AA senses B , although it is difficult to define (Sanchez Almeida et al. 1996) and, in fact, varies from point to point over the solar surface. The height of this layer corresponds to $z = 0$ in Fig. 1.

To get a first impression of the 3D magnetic field structure in the chromosphere and corona we extrapolate the photospheric measurements into the atmosphere under the force-free assumption.

$$\nabla \times \mathbf{B} = \alpha \mathbf{B} \quad (1)$$

$$\nabla \cdot \mathbf{B} = 0 \quad (2)$$

$$\mathbf{B} = \mathbf{B}_{\text{obs}} \text{ in photosphere,} \quad (3)$$

where \mathbf{B} is the magnetic flux density and α is the force-free parameter. Here we use mainly potential field extrapolations ($\alpha = 0$) due to the

generally low signal level in the quiet Sun, in particular of the linear polarization. Taking into account the non-force-free character of photosphere and lower chromosphere (as, e.g., proposed in Petrie & Neukirch 2000; Wiegmann & Neukirch 2006) require information on the plasma density and temperature distribution. The employed approximation is supported by spectro-polarimetric observations from Martínez González et al. (2010), which suggest that quiet sun loops show a potential field like structure. We solve equations (1)-(3) with the help of a fast Fourier approach (see Alissandrakis 1981) with the measured vertical magnetic field as boundary condition. A Fourier approach is justified because the magnetogram is almost flux balanced with $\sum_{x,y} B_z / \sum_{x,y} |B_z| = -0.077$. The computations are carried out in a cubic box with $936 \times 936 \times 468$ grid points in x, y, z , where z is the vertical direction. We use a constant grid resolution of 40 km in each direction, which corresponds to a total 3D model volume of $37 \times 37 \times 19$ Mm. Figure 1a shows the line-of-sight photospheric magnetic field and slices of the reconstructed magnetic field at different heights in the solar atmosphere in Fig. 1b-d. With increasing height in the solar atmosphere the magnetic field becomes smoother and shows a dipolar structure at coronal heights.

3. Statistics of magnetic loops.

We compute magnetic field lines from all pixels above a certain threshold value, here $|B_z| > 30$ G in the photosphere, which corresponds to the 3σ noise level of the magnetogram. The field line integration is started in a rectangular area at the center of the magnetogram, 150 pixels or 6 Mm away from the lateral boundaries. A total of 28005 field lines are followed from one foot point to the other. Of these 1936 (7%) leave the computational domain through the lateral or top boundaries. We cannot say if these lines are really open or close outside the SUNRISE/IMaX FOV. Consequently, we do not consider them further in this section. For simplicity we call closed magnetic field lines *loops* for the rest of this paper. Such magnetic loops are ubiquitous in the solar atmosphere, although only a fraction of these loops might be visible in images made in chromospheric, transition region or coronal radiation. Loops with a height

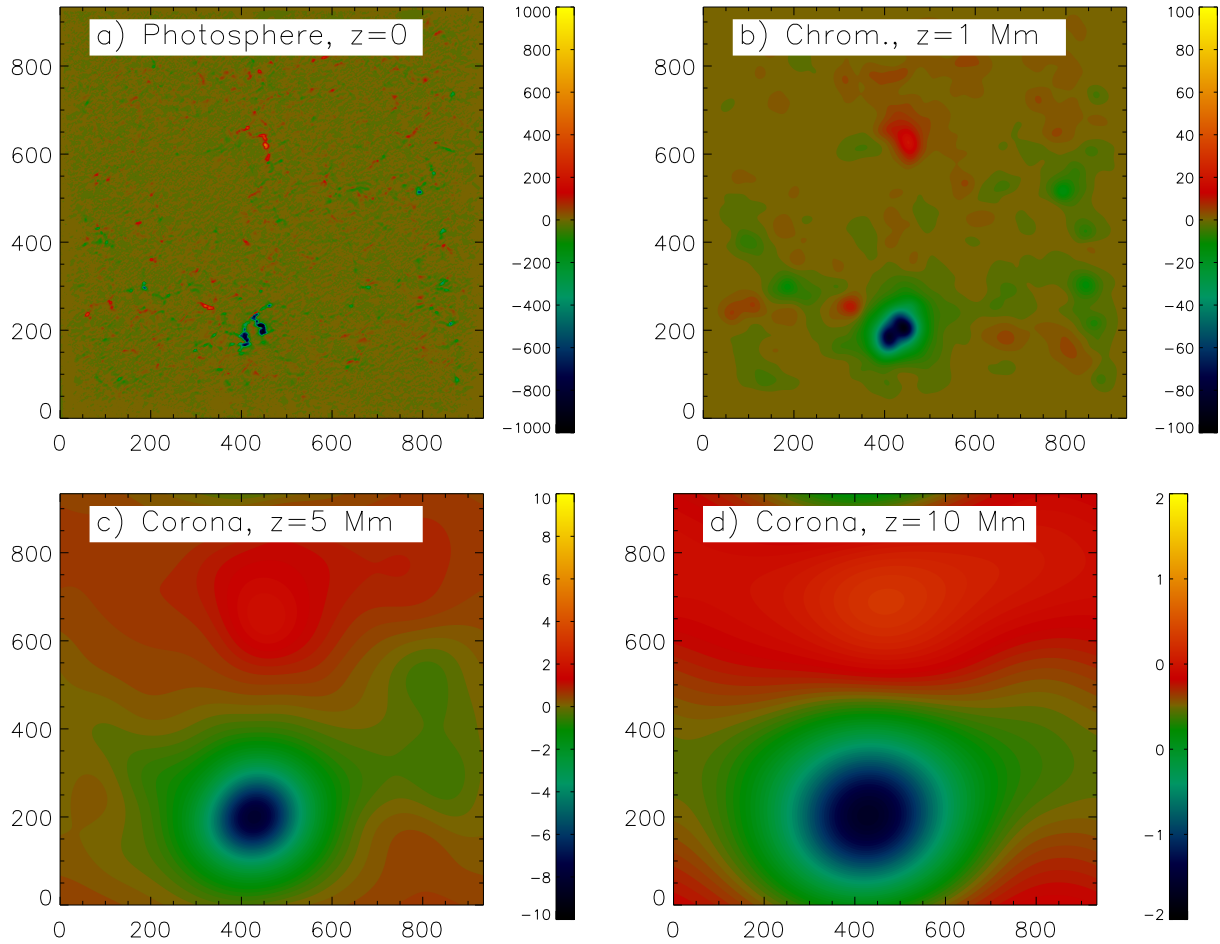


Fig. 1.— Vertical magnetic field at different heights. Panel a) shows the measured magnetogram in the photosphere and panels b-d) the vertical magnetic field distribution in different heights in the solar atmosphere, as reconstructed with a potential field model. The colour bars show the magnetic field strength in G.

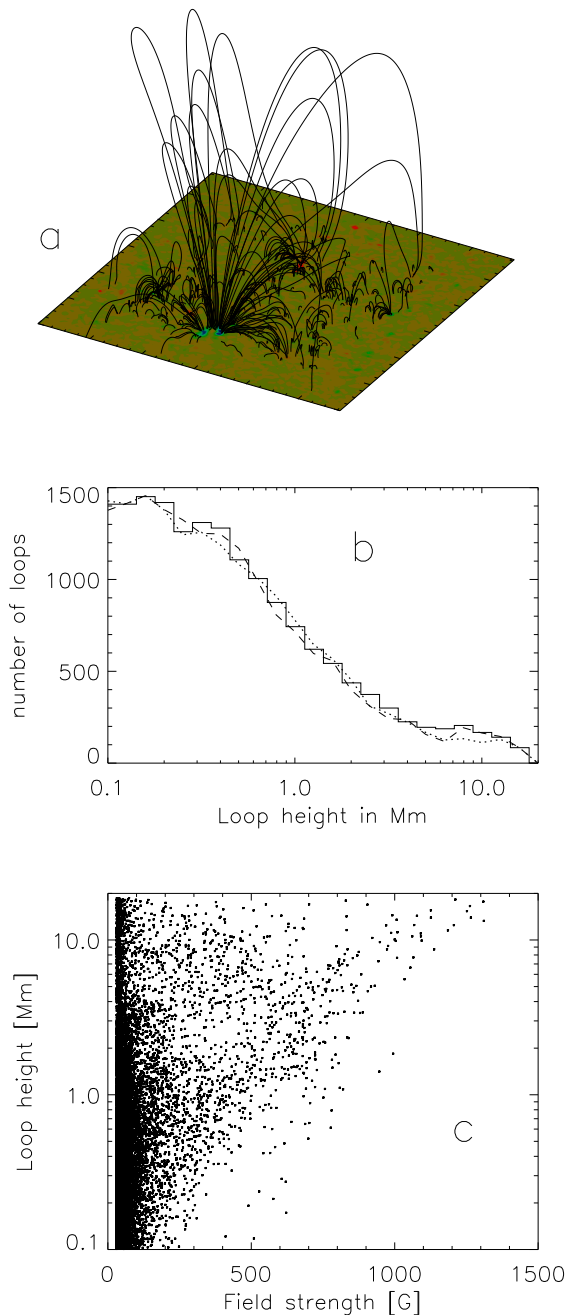


Fig. 2.— a) A random selection of 2% of magnetic loops, computed from a potential field reconstruction. b) Loop statistics for all resolved loops. The solid histogram-style line corresponds to a potential field and the dotted and dashed lines to a linear force-free model with $\alpha \cdot L = 4$ and -4 , respectively. c) Scatter plot of loop height vs. leading foot point vertical field.

of less than 100 km (9321, 33% of all field lines), may not be spatially sufficiently resolved and are not considered further, leaving 16748 field lines (60% of all) to be studied.

Figure 2a shows a randomly chosen fraction of 2% of these loops and Fig. 2b a histogram of the loop height distribution for all resolved loops. The average loop height is 1.24 ± 2.45 Mm¹. The number of small loops (below about 1 Mm) is significantly larger than that of higher loops. 51% of the resolved loops² close within photospheric heights (< 500 km) and 29% in the chromosphere (500 – 2500 km). Finally 20% of the loops reach into the corona (> 2500 km), but half of these long coronal loops do not close within the Sunrise FOV.

We also investigated how using a linear force-free model instead of a potential field model influences the loop height statistics. These models contain the force-free parameter α , which cannot be deduced from the available data. Consequently one unique linear force-free model cannot be computed. To investigate the influence of linear electric currents, we carried out computations with $\alpha L = \pm 4$, respectively, where $L = 37$ Mm is the size of the employed portion of the magnetogram (see dotted and dashed lines in Fig. 2b, respectively). 4 is already quite a large value for the normalized force-free parameter αL and close to the mathematical allowed maximum value of $|\alpha L| = \sqrt{2\pi}$ (see discussion in Seehafer 1978, for a suitable rank of α -values for linear force-free models). As visible in Fig. 2b the loop height statistics are almost identical to those obtained from potential fields. Small differences occur only for field lines higher than about 5 Mm. For our study, which mainly concentrates on lower chromospheric loops, it is therefore justified to consider only potential fields.

Figure 2c contains a scatter plot of loop height vs. magnetic field strengths at the leading foot point, i.e. the foot point with the largest field strength. It shows that loops of any height can begin from weak fields, but only long loops start from strong-field foot points. This means that

¹For higher (lower) threshold values of $|B_z|$ the number of small loops decreases (increases), which affects the average loop height, e.g., to 1.38 Mm and 1.09 Mm for a threshold of 40 G and 20 G, respectively.

²All loops higher than 100 km, including the ones not closing within the Sunrise/IMaX FOV.

the stronger field ($|B_z| \gtrsim 800$ G) loops are all long enough to reach into the solar corona, whereas the apex of a loop originating in a weaker field region can lie in the photosphere, chromosphere or corona.

4. On the origin of chromospheric magnetic fields and magnetic energy

In the following we investigate in more detail the origin of magnetic fields in the mid-chromosphere at a height of 1 Mm and are in particular interested in the magnetic connectivity with photospheric fields. To this aim we start the magnetic field line integration in the chromosphere (see Fig. 1b) at every pixel except in a layer of 150 pixels towards the magnetogram boundaries. We track all field lines down to the photosphere and determine here in particular the leading, stronger photospheric foot points³. From this foot point map we can then distinguish between photospheric pixels hosting magnetic loops reaching into the chromosphere or higher and pixels not hosting such loops. Figure 3a shows the magnetic field strength distribution $|B_z|$ in the photosphere. The solid line is for all pixels, the dashed line for pixels hosting foot points of field lines that reach to a height of at least 1 Mm and the dotted line for pixels not hosting such loops. Above 500G the solid and dashed lines are practically identical and nearly all pixels above 500G host footpoints of chromospheric loops. For weak fields (< 100 G) only about 2% of the pixels host chromospheric loops, but the total number of these (hosting) pixels is still more than one order of magnitude higher than strong field pixels. This raises the question, which photospheric fields can influence the chromospheric and coronal gas more strongly, the few regions with strong fields or the many regions with weak fields? To answer this question we compute the magnetic energy at a height of 1 Mm and investigate which fraction of the energy is magnetically connected to photospheric foot points with a particular field strength. As one can see in Fig. 3b the weak

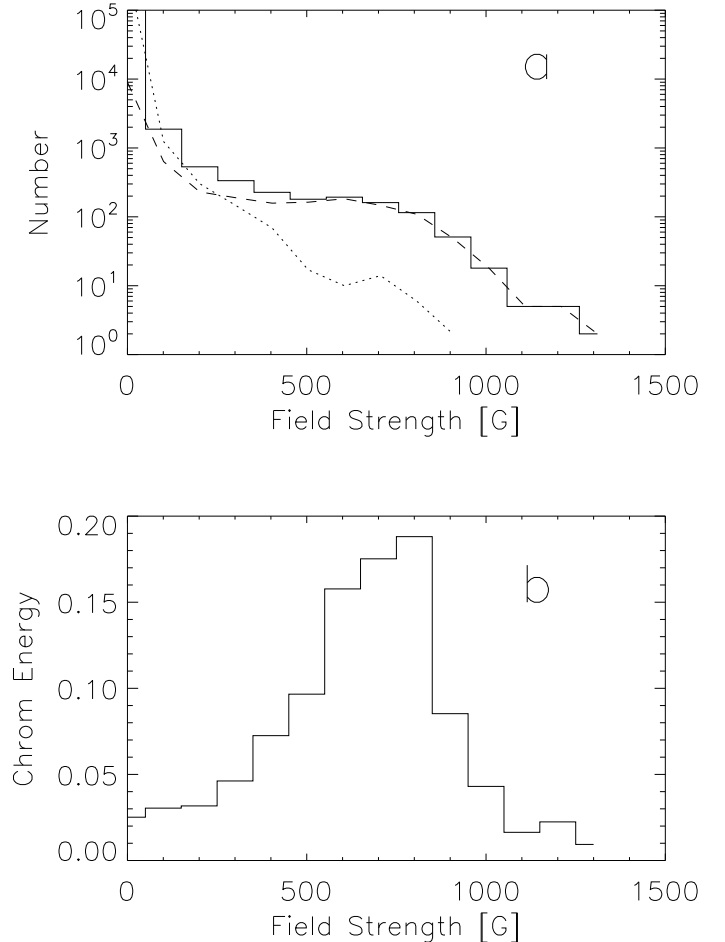


Fig. 3.— a) Photospheric field strength $|B_z|$ statistics of the photospheric magnetogram (excluding the 150 pixel layer towards the boundaries). The solid histogram-style line corresponds to all photospheric pixels, the dashed line to pixels hosting foot points of field lines reaching at least to 1 Mm, i.e. into the mid-chromosphere, and the dotted line to pixels not hosting such field lines. b) Histogram showing the fraction of magnetic energy at a height of 1 Mm (mid-chromosphere) in loops with a particular field strength of their leading foot point.

³Some long field lines do not close within the Sunrise-FOV and for them we can only identify one foot point. For the analysis in this section these field lines are included in the statistics assuming that the known foot point is the stronger one. The relation to the weaker foot points is investigated in section 5.

photospheric fields ($< 100\text{G}$) hardly contribute to chromospheric magnetic energy. In addition, although only 0.91% of all photospheric pixels have a field strength above 100 G, they are connected to 97% of the chromospheric magnetic energy. The 0.32% of pixels above the equipartition field strength of 300 G contribute to 91% of the chromospheric magnetic energy. At the equipartition field strength (which is in the range of 200-400G in the photosphere, see Solanki et al. 1996) the magnetic energy is identical to the energy of the convective flow. The equipartition field strength has relevance for quiet Sun magnetic features, because magnetic flux tubes need to have a larger field strength in order to survive as a distinct feature. It is therefore natural to distinguish network elements from internetwork features by the equipartition field strength. Here we used the average value of 300G.

Note that the photospheric field strength values are based on single component inversions assuming spatially resolved fields and are consequently lower limits (for the stronger field, they are close to the true value, see Lagg et al. 2010), and so are the above energy fractions of the chromospheric magnetic energy. The above numbers refer to the leading (stronger) foot point.

5. Relation between the two foot points of magnetic loops

In the last section we learned that 91% of the mid-chromospheric magnetic energy is topologically connected to photospheric foot points with superequipartition field strength. However, still unknown is if both foot points of long chromospheric and coronal loops have similar field strength or if it can be very different. If the latter is the case this would also mean that the multiple field lines starting within the area of a strong magnetic pixel will end in many, possibly widely distributed weak-field pixels ⁴. In Fig. 4a we show a scatter plot of weak foot point strength vs. strong foot point strength. ⁵. 95% of all loops

⁴In order to fulfill $\nabla \cdot \mathbf{B} = 0$ we get the relation $B_1 A_1 = B_2 A_2$ for the foot point areas A_1 and A_2 of magnetic flux tubes containing a bundle of field lines.

⁵Necessarily, we had to exclude those field lines which do not close within the Sunrise-FOV, because we cannot identify both foot points for them.

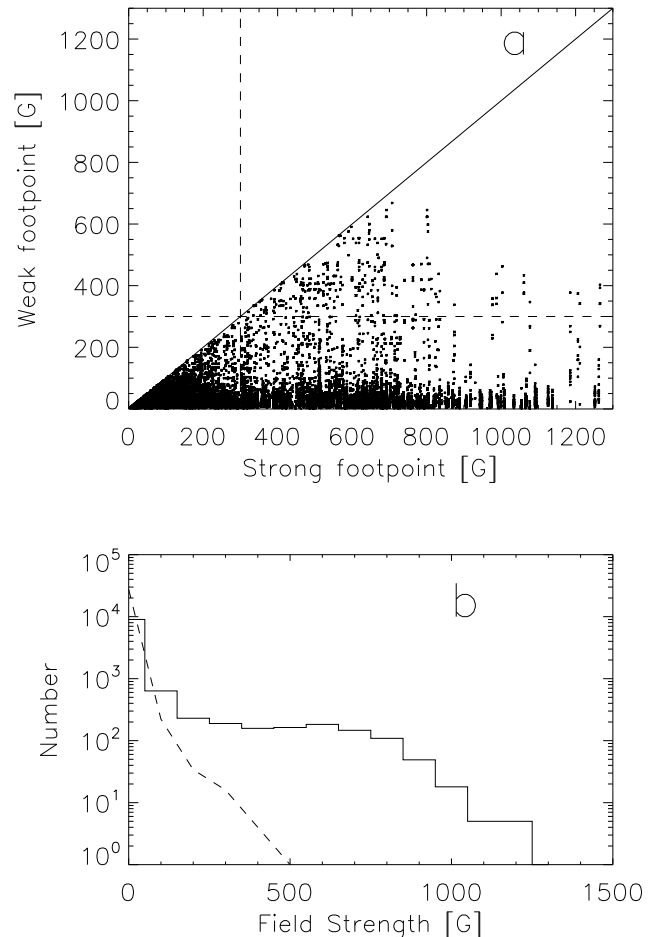


Fig. 4.— Relation between strong and weak foot points of magnetic loops which reach at least into the chromosphere. Excluded have been loops that do not close within the Sunrise-FOV (14%), because the strength of one foot point remains unknown. Panel a) shows a scatter plot of weak foot point strength vs. strong foot point strength. The solid diagonal line corresponds to equal strength of both foot points and the dashed horizontal and vertical lines mark the equipartition field strength of 300 G. Panel b): Photospheric field strength $|B_z|$ statistics for the strong (solid line) and weak foot points (dashed line) of chromospheric and coronal loops.

with a leading foot strength of > 300 G, have the other foot point in regions with < 300 G. Figure 4b shows the photospheric vertical field $|B_z|$ statistics for pixels hosting a leading (stronger) foot point (solid histogram-style line) and for pixel hosting a weak foot point (dashed line). Obviously the vertical field of both foot points for long loops (reaching at least into the chromosphere) is very different. Partly, this has to do with the different field strength distribution in the two magnetic polarities for this particular magnetogram. The maximum vertical field in the negative field region is 1311 G, compared to 707 G in positive polarity regions⁶. Investigations of further quiet Sun regions with high resolution are necessary to see if such different field strengths are common or an exception (For quiet Sun investigations of magnetic flux see, e.g. Wang et al. 1995).

6. Conclusions and outlook

We investigated the small-scale structure of magnetic fields in the solar atmosphere with emphasis on the magnetic connectivity between the photosphere and chromosphere. We found that chromospheric areas containing about 91% of the magnetic energy are topologically connected to a photospheric foot point with a strength above 300 G, i.e. with an energy density higher than the average equipartition with that of convective flows. For the majority of the loops the magnetic field strength in both foot points differs significantly, with the second foot point having a field strength below equipartition, i.e. network elements connect magnetically mainly to internetwork (IN) features, in general agreement with numerical experiments of Schrijver & Title (2003); Jendersie & Peter (2006). An interesting question is to which extent the finding that network elements are connected mainly with IN features might influence models of quiet-Sun loop heating (e.g., Hansteen 1993; Chae et al. 2002; Müller et al. 2003, 2004). Such loop heating models usually assume a constant cross section, an approximation which is not fulfilled for field lines connecting strong and weak field regions in the

photosphere. It is also worth noting that IN fields are more dynamic and short-lived than network fields (IN field average lifetimes are about 10 min according to de Wijn et al. 2008). Since most chromospheric and coronal loops, at least in the observed region, are connected at one foot point with IN fields we expect the chromospheric and coronal field to be more dynamic than suggested by network fields alone. Time series of high resolution magnetograms in the quiet Sun can be used to investigate this further and to revisit *coronal recycling* (e.g., as investigated at much lower spatial resolution by Close et al. 2004, 2005).

The German contribution to *Sunrise* is funded by the Bundesministerium für Wirtschaft und Technologie through Deutsches Zentrum für Luft- und Raumfahrt e.V. (DLR), Grant No. 50 OU 0401, and by the Innovationsfond of the President of the Max Planck Society (MPG). The Spanish contribution has been funded by the Spanish MICINN under projects ESP2006-13030-C06 and AYA2009-14105-C06 (including European FEDER funds). The HAO contribution was partly funded through NASA grant number NNX08AH38G. This work has been partially supported by the WCU grant No. R31-10016 funded by the Korean Ministry of Education, Science and Technology.

REFERENCES

- Alissandrakis, C. E. 1981, *A&A*, 100, 197
- Barthol, P., Gandorfer, A., Solanki, S. K., et al. 2010, *Sol. Phys.*, submitted
- Bello González, N., Flores Soriano, M., Kneer, F., & Okunev, O. 2009, *A&A*, 508, 941
- Bello González, N., Franz, M., Martínez Pillet, V., et al. 2010, *ApJL*, this issue
- Borrero, J. M., Tomczyk, S., Kubo, M., et al. 2010, *Sol. Phys.*, 35
- Carlsson, M., Hansteen, V. H., de Pontieu, B., et al. 2007, *PASJ*, 59, 663
- Chae, J., Poland, A. I., & Aschwanden, M. J. 2002, *ApJ*, 581, 726
- Close, R. M., Parnell, C. E., Longcope, D. W., & Priest, E. R. 2004, *ApJ*, 612, L81

⁶Indirect evidence of large network fields of 1-2 kG concentrated in small regions has been given already in Tarbell & Title (1977), but the magnetograph resolution of that time has been too low to resolve such structures.

- Close, R. M., Parnell, C. E., Longcope, D. W., & Priest, E. R. 2005, *Sol. Phys.*, 231, 45
- Danilovic, S., Lagg, A., Pietarila, A., et al. 2010, this issue
- de Wijn, A. G., Lites, B. W., Berger, T. E., et al. 2008, *ApJ*, 684, 1469
- Hansteen, V. 1993, *ApJ*, 402, 741
- He, J., Tu, C., & Marsch, E. 2007, *A&A*, 468, 307
- Jendersie, S. & Peter, H. 2006, *A&A*, 460, 901
- Lagg, A., Solanki, S. K., Riethmüller, T. L., et al. 2010, *ApJL*, this issue
- Martínez González, M. J. & Bellot Rubio, L. R. 2009, *ApJ*, 700, 1391
- Martínez González, M. J., Collados, M., Ruiz Cobo, B., & Beck, C. 2008, *A&A*, 477, 953
- Martínez González, M. J., Manso Sainz, R., Asensio Ramos, A., & Bellot Rubio, L. R. 2010, *ApJ*, 714, L94
- Martínez Pillet, V., Bonet, J. A., Collados, M., et al. 2010, *Sol. Phys.*, submitted
- Müller, D. A. N., Hansteen, V. H., & Peter, H. 2003, *A&A*, 411, 605
- Müller, D. A. N., Peter, H., & Hansteen, V. H. 2004, *A&A*, 424, 289
- Petrie, G. J. D. & Neukirch, T. 2000, *A&A*, 356, 735
- Sanchez Almeida, J., Ruiz Cobo, B., & del Toro Iniesta, J. C. 1996, *A&A*, 314, 295
- Schrijver, C. J. & Title, A. M. 2003, *ApJ*, 597, L165
- Seehafer, N. 1978, *Sol. Phys.*, 58, 215
- Solanki, S. K., Barthol, P., Danilovic, S., et al. 2010, *ApJL*, this issue
- Solanki, S. K., Zufferey, D., Lin, H., Rüedi, I., & Kuhn, J. R. 1996, *A&A*, 310, L33
- Tarbell, T. D. & Title, A. M. 1977, *Sol. Phys.*, 52, 13
- Wang, J., Wang, H., Tang, F., Lee, J. W., & Zirin, H. 1995, *Sol. Phys.*, 160, 277
- Wiegelmann, T. & Neukirch, T. 2006, *A&A*, 457, 1053
- Wiegelmann, T. & Solanki, S. K. 2004, *Sol. Phys.*, 225, 227